CRYSTAL STRUCTURE EFFECT ON METALLIC MECHANICAL PROPERTIES OF UNDER TENSION STRESS: MOLECULAR DYNAMICS STUDY

Ming Wang[1, 2], Yonghao Zeng[1], Ying Chen[1], Shiyi Zhang[1]
[1]School of Materials Science and Engineering, Liaoning Technical University, P.R. China;
[2]Key Laboratory of Mineral High Value Conversion and Energy Storage Materials of Liaoning Province, P.R. China
mwang.lntu@hotmail.com

Abstract. In the paper, the tensile mechanical properties and deformation behaviour of different crystal structures (face-centered cubic (FCC) metal ~Al and closely packed hexagonal (HCP) metal ~Ti) were studied using molecular dynamics calculation through the LAMMPS module of Materials and Processes Simulations (MAPS) software, and the effect of microstructure on their mechanical properties was explored from the atomic level, in order to reveal the deformation mechanism of different lattice types of metals at the atomic scale. The simulation results using MAPS showed that the elastic modulus and the tensile strength of Al was calculated with 45.0 GPa and 6.2 GPa, respectively, the flow stress of Al has a stable value of around 0.69-1.29 GPa. And the elastic modulus and the tensile strength of Ti was calculated with 73.1 GPa and 8.5 GPa, respectively. According to calculation by Ovite, the occurrence of dislocations in Ti was later than that in Al, indicating that the strain energy that can be accumulated in the Ti lattice of HCP structure was higher and the ability to resist deformation was greater. As the periodic boundary conditions were used in all three directions of the two model, there was no macroscopic breaking phenomenon. To sum up, the lattice of HCP structure (~Ti) can accumulate higher strain energy and have greater deformation resistance ability than that of FCC structure (~Al), which was the reason for the elastic modulus and tensile strength of Ti higher than those of Al.

Keywords: molecular dynamics, crystal structure, mechanical properties.

Introduction

Metals have extremely important applications in the field of construction, the study of their mechanical properties can effectively reduce losses, the study of new alloys with high strength and good plasticity can also promote the development of industry and promote social progress. The elastic modulus of metals is considered as the ability of objects to resist elastic deformation, and from a microscopic point of view, it is a reflection of the bonding strength between atoms, ions or molecules [1]. With the development of computer calculation technology, molecular dynamics simulation has been widely used in material science research. In recent years, many researchers have done a lot of research on the mechanical properties and microstructure evolution of metals by molecular dynamics methods [2-10]. Zhu and Shi [7] presented the reorientation and pseudoplasticity in Fe nanowires induced by compression strain and found an intricate temperature dependence of the reorientation. To investigate the effect of different boundary conditions on tensile fracture process, Chen et al. [9] performed uniaxial tensile test of Cu by molecular dynamics simulations. The results show that the elastic modulus of nanocrystalline Cu with grain sizes of 4.65-12.41 nm gradually increases with the increase of the mean grain sizes, the corresponding flow stress concurrently increases, and the flow stress is proportional to the square-root of the grain size, which satisfies the inverse-Hall–Petch relation. Furthermore, the elastic modulus linearly decreases with the increase of temperature. The coupled effect of the flow stress, strain rate and temperature were elaborated by the Arrhenius hyperbolic sinusoidal model. Meanwhile, the deformation activation energy of nanocrystalline Cu for various grain sizes was obtained. Imran et al. [10] used three-dimensional molecular dynamics simulation to elucidate the nanoindentation behaviour of single crystal Ni.

MAPS software is a multi-scale, multi-paradigm and extensible platform to facilitate the modeling of real models of all types of materials, and the software uses the world's leading simulation tools to simulate various properties and chemical processes, making it easy to analyze key properties and then predict and screen the behaviour of materials under different conditions.

In this work, the tensile mechanical properties and behavior of Al and Ti according to the LAMMPS module in MAPS was investigated, the change of the stress-strain curve of Al and Ti was discussed from the atomic level, and the microstructure effect on their mechanical properties was studied.

Simulation methods

The model sizes of Al and Ti were both $10a_0 \times 10b_0 \times 10c_0$, and their lattice constants were $a_{Al} = b_{Al} = c_{Al} = 4.05$ Å and $a_{Ti} = b_{Ti} = 2.95$ Å, $c_{Ti} = 4.686$ Å, respectively at room temperature [11-12]. There were total 4000 atoms in the Al model, the actual size of the model was $4.05 \times 4.05 \times 4.05$nm; and, there were 2000 atoms in the Ti model, and the actual size was $2.95 \times 2.95 \times 4.686$nm. The three directions of X, Y and Z in the two models were the same, which were [100]×[010]×[001] phases, respectively, and the atomic plane (111) was parallel to Ti (0001).

The initial models for Al and Ti were selected eam/alloy [13] and eam/fs [14] potential functions, respectively. The relaxed structure was obtained after the equilibrium at 298 K and 0 atm using the isothermal-isobaric (NPT) ensemble [15] with the Nose-Hoover thermostat and the Nose/Hoover pressure barostat for 20 ps. The models were loaded using the deform command that changed the volume of the simulation box during running a dynamics simulation and stretched it in the X-direction with a constant strain rate. The standard Velocity-Verlet algorithm was implemented to integrate Newton's equation of motion, where the time step was set at 1 fs. During loading, the isothermal-isobaric (NPT) system ensemble was utilized to update the positions and velocities of the atoms to obtain the prescribed structure.

Results and discussion

The stress-strain curves of Al and Ti can be obtained by molecular dynamics simulation as shown in Figure 1.
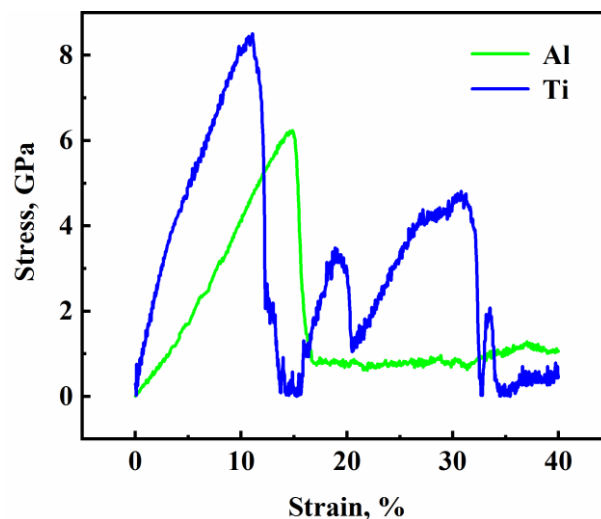

Fig. 1. **Stress-strain curve of Al and Ti**

The atomic trajectory information was processed by Ovito, and the drawing process diagram of Al and Ti special time system is shown in Figure 2.

From Figure 1, the Al stress-strain curve can be divided into three stages. (I) Ascending stage, the stress increased linearly with the strain. Before the strain reached 14.8%, the range of Al was the elastic deformation stage. In this stage, the stress-strain curve was approximately a straight line, and the stress increased linearly with the strain. According to Hooke's law [16], it was calculated that the elastic modulus of Al was 45.0 GPa (the error with the reported value [17] is within the allowable range). Before the strain of Al reached 14.8%, the simulation system expanded approximately uniformly, there was a small movement in the atomic position, the microcracks did not develop obviously, and there were no micro voids as a whole stage, corresponding to Figure 2 (a). (II) Descending part, the stress decreased with the increase of strain. When the strain of Al reached 14.8%, the stress reached the peak value of 6.2 GPa. Then, with the increase of the strain, the stress decreased sharply, and when the strain energy accumulated in the lattice was too high, dislocation release strain energy was emitted at the crack tip, corresponding to Figure 2 (b)-(d). (III) Stationary part, the stress fluctuated up and down with the increase of the strain. As the three directions of the model used periodic boundaries, which was equivalent to simulating an infinite system, there was no macroscopic breaking phenomenon, so there

was still considerable stress after ε = 17.1%, the flow stress of Al had a stable value of around 0.69-1.29 GPa.

Compared with the reported stress-strain curve of Ti [18], the calculated stress-strain curve in this work is not much different from that reported curve. According to the Ti stress-strain curve, before the strain reached 11.1%, the range of Ti can be regarded as the stage of elastic deformation. In this stage, the stress-strain curve was similar to a straight line, and the stress increased linearly with the strain. The elastic modulus of Ti was 73.1 GPa. Before the strain of Ti reached 11.1%, the simulation system expanded approximately uniformly, there was a small movement in the atomic position, the microcracks did not develop obviously, and there were no holes, corresponding to Figure 2 (e). When the strain of Ti reached 11.1%, the stress reached the peak value of 8.5 GPa. After that, with the continuation of tension stress, when the accumulated strain energy in the lattice was high enough, the dislocation was emitted at the crack tip accompanied with strain energy release. Corresponding to Figure 2 (f)-(g), the stress decreased with the increase of strain in Figure 2(b). With the increase of the strain, the stress increased to the peak value for the second time, as shown in Figure 1, which indicated the second hardening under tensile load. As the periodic boundary conditions were used in all three directions of the model, there was no macroscopic breaking phenomenon.
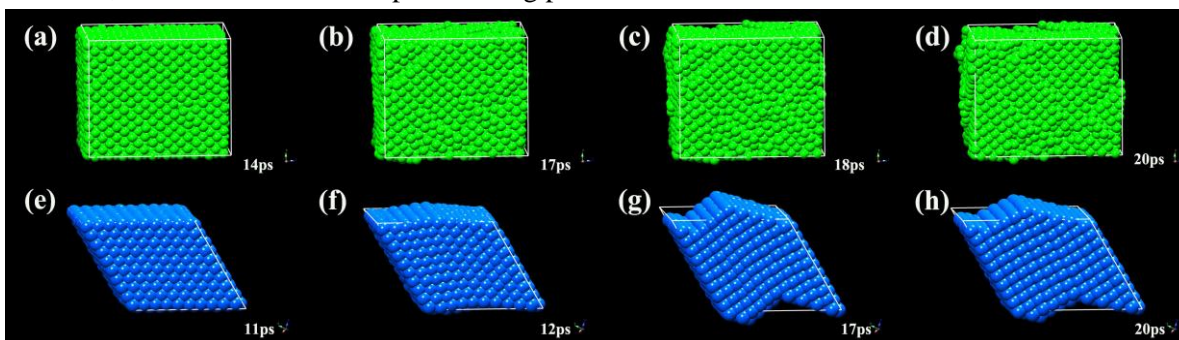

Fig. 2. **Tensile process of system at special moment:** a-d – Al; e-h – Ti

The evolution of the percentage of phase composition in the system is shown in Figure 3. According to Figure 3 (a), the decrease of Al stress-strain curve was caused by the decrease of FCC phase content when the strain was about 14%. With the nucleation of dislocations, the percentage of unrecognized (other) atoms began to decrease, and the FCC and HCP phases increased. With the increase of the tensile load, the phase transformation between other, HCP and FCC structures led to stress fluctuation in the process of plastic deformation. According to Figure 3 (b), in the early stage of tension, the structure of Ti was HCP. When the strain reached 11%, the decrease of the HCP phase content led to the decrease of the stress-strain curve. When the strain reached 17%, the content of HCP phase began to increase and the content of unrecognized (other) phase decreased, resulting in a secondary increase in the elastic modulus of Ti. According to Figure 1 and Figure 3, the tensile strength of FCC was lower than that of the HCP phase.
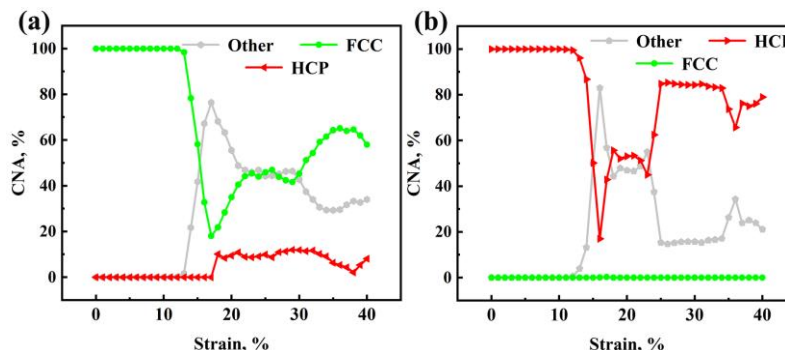

Fig. 3. **Evolution of phase percentages:** a – Al; b – Ti

The distribution of dislocation in Al and Ti systems is shown in Figure 4. It can be seen from Figure 4 (a)-(d) that the dislocations in the Al model began to appear in 14 ps and suddenly increased at 17ps, corresponding to the appearance of the HCP phase. The density of these dislocations increased

sharply after the strain reached 17% and tended to stabilize after the strain was about 22%. There was no dislocation in the model Ti before 17 ps, the other dislocation began to appear during 17ps. At this time, the other was transformed into the HCP phase transition. There was a phase transition in 24 ps, the content of the other phase decreased and the HCP phase increased, resulting in the dislocation of $1/3 < 1\,\bar{2}10 >$ evolved. The occurrence of dislocations in Ti was later than that in Al, indicating that the strain energy that can be accumulated in the Ti lattice of HCP structure was higher and the ability to resist deformation was greater.
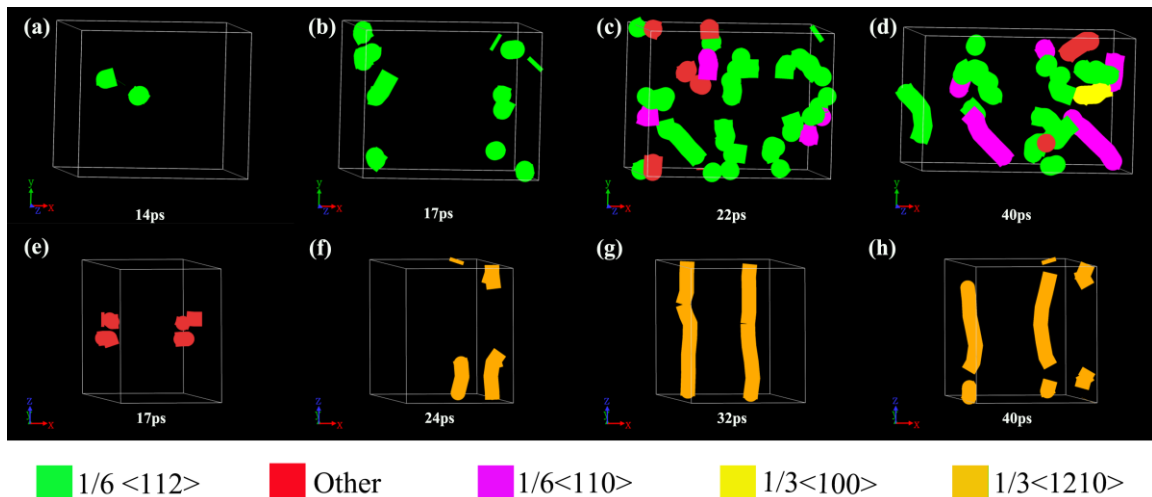

Fig. 4. **Distribution of dislocation:** (a)~(d)-Al; (e)~(h)-Ti

Conclusions

In this paper, the tensile mechanical properties and behaviour of Al and Ti were calculated by LAMMPS module in MAPS software. Through simulation calculation, the elastic modulus and the tensile strength of Al was calculated with 45.0 GPa and 6.2 GPa, respectively, the flow stress of Al has a stable value of around 0.69-1.29 GPa. And the elastic modulus and the tensile strength of Ti was calculated with 73.1 GPa and 8.5 GPa, respectively. The lattice of Ti (HCP) can accumulate higher strain energy and have a greater deformation resistance ability than that of Al (FCC), so the elastic modulus and tensile strength of Ti were higher than those of Al.

Acknowledgements

Author contributions

Conceptualization, M. Wang; methodology, M. Wang and Y.H. Zeng; software, Y.H. Zeng; investigation, Y. Chen and S.Y. Zhang; data curation, Y.H. Zeng; writing – original draft preparation, Y.H. Zeng.; writing – review and editing, M. Wang, Y.H. Zeng, Y. Chen and S.Y. Zhang; funding acquisition, M. Wang.

References

[1] Dadrasi A., Albooyeh A.R., Mashhadzadeh A.H. Mechanical property of silicon-germanium nanotubes: A molecular dynamics study. Applied Surface Science, vol. 498, 2019, pp. 143867.
[2] Xu L., Huang Z., Shen Q., et al. Atomistic Simulations of Plasticity Heterogeneity in Gradient Nano-grained FCC Metals. Materials & Design, vol. 221, 2022, pp. 110929.
[3] Deng X., Xiao Y., Ma Y., et al. The Microstructural Evolution of Nickel Single Crystal under Cyclic Deformation and Hyper-Gravity Conditions: A Molecular Dynamics Study. Metals, vol. 12, 2022, pp. 1128.

[4] Souq S.M.N, Ghasemi F.A, Fakhrabadi M.M.S. Effects of Various Cross Sections on Elastoplastic Behavior of Fe Nanowires under Tension/Compression. Journal of Materials Engineering and Performance, vol. 32, 2022, pp. 1-15.

[5] Zhao D., Zhu B., Wang S., et al. Effects of pre-strain on the nanoindentation behaviors of metallic glass studied by molecular dynamics simulations. Computational Materials Science, vol. 186, 2021, pp. 110073.

[6] Kedharnath A., Kapoor R., Sarkar A. Classical molecular dynamics simulations of the deformation of metals under uniaxial monotonic loading: A review. Computers & Structures, vol. 254, 2021, pp. 106614.

[7] Zhu J., Shi D. Reorientation mechanisms and pseudoelasticity in iron nanowires. Journal of Physics D: Applied Physics, vol. 44(5), 2011, pp. 055404.

[8] Li S., Liu Y., Ye H., et al. Sintering mechanism of Ag nanoparticle-nanoflake: a molecular dynamics simulation. journal of materials research and technology, vol. 16, 2022, pp. 640-655.

[9] Chen P., Zhang Z., Liu C., et al. Temperature and grain size dependences of mechanical properties of nanocrystalline copper by molecular dynamics simulation. Modelling and Simulation in Materials Science and Engineering, vol. 27, 2019, pp. 065012.

[10] Imran M., Hussain F., Rashid M., et al. Dynamic characteristics of nanoindentation in Ni: A molecular dynamics simulation study. Chinese Physics B, vol. 21, 2012, pp. 116201.

[11] Mendelev M.I., Kramer M.J., Becker C.A., et al. Analysis of semi-empirical interatomic potentials appropriate for simulation of crystalline and liquid Al and Cu. Philosophical Magazine, vol. 88, 2008, pp. 1723-1750.

[12] Gholizadeh P., Amini H., Davoodi J., et al. Molecular dynamic simulation of crack growth in Ti/TiN multilayer coatings. Materials Today Communications, vol. 30, 2022, pp. 103059.

[13] Zhou X.W., Johnson R.A., Wadley H.N.G. Misfit-energy-increasing dislocations in vapor-deposited CoFe/NiFe multilayers. Physical Review B, vol. 69, 2004, pp. 144113.

[14] Mendelev M.I., Underwood T.L., Ackland G.J. Development of an interatomic potential for the simulation of defects, plasticity, and phase transformations in titanium. The Journal of chemical physics, vol. 145, 2016, pp. 154102.

[15] Guo W., Zeng L., Lu Y., et al. Tuning surface hybrid-wettability to enhance the vapour film phenomenon induced by boiling heat transfer: Molecular dynamics. International Communications in Heat and Mass Transfer, vol. 136, 2022, pp. 106172.

[16] Hosseini A., Nasrabadi M.N. Investigation of vacancy defects and temperature effects on the GaN bombarding with argon atoms: Molecular dynamics simulation. Materials Chemistry and Physics, vol. 271, 2021, pp. 124854.

[17] Yousefi E., Sun Y., Kunwar A., et al. Surface tension of aluminum-oxygen system: A molecular dynamics study. Acta Materialia, vol. 221, 2021, pp. 117430.

[18] An M., Deng Q., Li Y., et al. Molecular dynamics study of tension-compression asymmetry of nanocrystal α-Ti with stacking fault. Materials & Design, vol. 127, 2017, pp. 204-214.